
FSDAM: FEW-SHOT DRIVER ATTENTION MODELING VIA VISION-LANGUAGE COUPLING

Kaiser Hamid

Texas Tech University, Lubbock, TX
mdmunna@ttu.edu

Can Cui

Purdue University, West Lafayette, IN
cancui@purdue.edu

Khandakar Ashrafi Akbar, PhD

University of Texas at Dallas, Richardson, TX
kakbar@towson.edu

Ziran Wang, PhD

Purdue University, West Lafayette, IN
ziran@purdue.edu

Nade Liang

Texas Tech University, Lubbock, TX
nade.liang@ttu.edu

November 18, 2025

ABSTRACT

Understanding where drivers look and why they shift their attention is essential for autonomous systems that read human intent and justify their actions. Most existing models rely on large-scale gaze datasets to learn these patterns; however, such datasets are labor-intensive to collect and time-consuming to curate. We present **FSDAM** (Few-Shot Driver Attention Modeling), a framework that achieves joint attention prediction and caption generation with approximately 100 annotated examples, two orders of magnitude fewer than existing approaches. Our approach introduces a dual-pathway architecture where separate modules handle spatial prediction and caption generation while maintaining semantic consistency through cross-modal alignment. Despite minimal supervision, FSDAM achieves competitive performance on attention prediction, generates coherent, and context-aware explanations. The model demonstrates robust zero-shot generalization across multiple driving benchmarks. This work shows that effective attention-conditioned generation is achievable with limited supervision, opening new possibilities for practical deployment of explainable driver attention systems in data-constrained scenarios.

1 Introduction

Driving is primarily a visual task. Drivers constantly move their gaze across different environmental elements, such as traffic signals, crossing pedestrians, and road hazards. This selective attention directly influences their understanding of the situation and decision-making process. Suboptimal attention allocation due to distraction or drowsiness remains a leading cause of accidents, with disproportionate crash rates at intersections where drivers fail to notice crossing traffic, or during lane changes when blind spots go unchecked [1, 2]. Understanding where and what drivers visually attend to can also be beneficial to Advanced Driver Assistance Systems (ADAS) and autonomous vehicles (AVs) operating in mixed-traffic environments, where human-AI collaboration depends on a shared perception of the surroundings. Modeling driver attention allows for cross-verification of the human-machine goal alignment by comparing human intention with decisions made by autonomous systems. This process validates whether the planned maneuvers are consistent with the perceived context of the scene, and it also supports interpretable decision-making chains that enhance user trust in human-AI collaboration.

Despite its importance, effectively modeling driver attention faces fundamental challenges. Existing approaches rely heavily on supervised learning that requires large, labeled eye-tracking data collected in well-represented conditions to

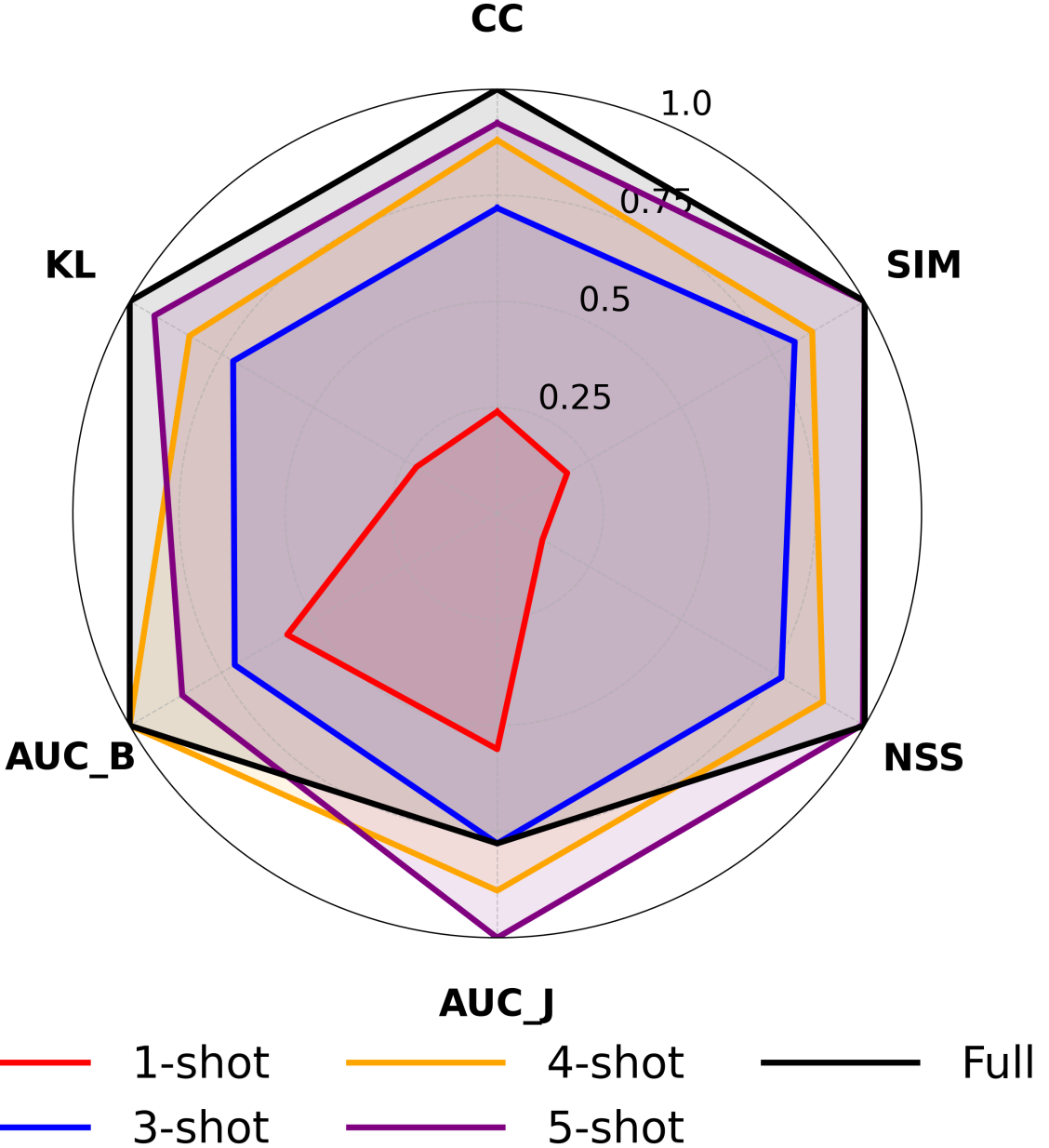


Figure 1: Few-shot learning performance on BDD-A dataset. Gaze prediction metrics: CC, SIM, NSS, AUC-J, AUC-B, and KL (inverted). All metrics are linearly min-max normalized to [0,1] where larger area indicates better performance.

provide stable inductive biases for low-level perception. However, the data collection and annotation can be costly and often lack diversity in safety-critical scenarios [3]. Additionally, an image dataset containing driver gaze information can expose sensitive biometric and behavioral data, potentially revealing individuals' identity and attention patterns [4]. This data scarcity, coupled with privacy and annotation costs, can lead to long-tail errors during domain-specific corner cases and rare events [5]. Moreover, the space of possible driving scenarios grows combinatorially with environmental factors, traffic configurations, and agent behaviors, making comprehensive coverage through dataset expansion increasingly impractical [5, 3]. These constraints necessitate a shift from data-hungry supervised learning to sample-efficient learning with semantic grounding. In addition to learning visual attention patterns through labeled datasets, semantic understanding of the surrounding environment can also benefit visual attention prediction. For example, knowing that "pedestrians near crosswalks" or "vehicles braking suddenly" are situations where driver attention is typically expected,

and can be encoded as an auxiliary loss that encourages the model’s attention distribution to place more weight on these regions. Vision-language models (VLMs) can offer this capability: their pre-trained representations encode rich semantic knowledge about objects, spatial relationships, and causal reasoning. Rather than learning attention patterns from scratch, VLMs can exploit these semantic priors to achieve few-shot generalization with as few as 5-32 examples per class [6]. In autonomous driving, works like DriveLM [7] have demonstrated that grounding perception in natural language enables more interpretable reasoning that generalizes across scenarios. Building on this insight, Zhou et al. [8] pioneered joint attention-language modeling with LLaDA, demonstrating that coupling spatial attention prediction with textual reasoning improves both quantitative performance and interpretability. Similarly, Chen et al. [9] showed that generating natural language explanations enhances gaze prediction understanding. While these works demonstrate the potential of vision-language models for joint spatial and semantic reasoning, they still require extensive labeling. The objective of this work is therefore to *leverage VLM priors to learn driver attention from fewer labeled examples*.

To address these limitations, we develop **FSDAM**, a framework that learns joint gaze prediction and attention-grounded caption generation from approximately 100 annotated examples. To our knowledge, *this is the first work to demonstrate that attention-conditioned language generation can be learned effectively in a few-shot regime*. Beyond data efficiency, we introduce attention shift anticipation: unlike prior work that describes current attention, our model predicts where drivers will look next from single frames. We create supervision by selecting frame pairs where attention demonstrably shifts and annotating observed transitions with structured captions describing scene context, current focus, anticipated shift, and causal reasoning. At inference, the model learns to anticipate these shifts from single frames alone, capturing the forward-looking nature of human attention without requiring video input. Our key insight is to structure the learning task so that spatial attention and language understanding provide complementary supervision signals. We introduce a structured attention reasoning representation where each annotation describes the driving scene, identifies where the driver is currently looking, predicts where attention will shift next, and explains why. This structured representation creates explicit connections between visual attention patterns and semantic reasoning.

Our architecture processes visual features through two pathways: one generates attention-grounded captions while the other aligns predicted attention with language representations. Both pathways share the same visual features but specialize for their respective tasks. Starting from approximately 100 training examples curated from the Berkeley DeepDrive Attention (BDD-A) dataset [10], our model achieves strong spatial attention prediction despite the severe data limitation. It reduces KL divergence on BDD-A by up to 89% compared to fully supervised baselines and delivers competitive CC and NSS values. Zero shot transfer experiments on DR(eye)VE [11] and DADA 2000 [12] further show that FSDAM maintains the lowest KL divergence and strong SIM scores across these unseen domains, indicating that the learned attention language alignment generalizes well beyond its training distribution. This efficient learning regime supports practical use in driving environments where gaze data is limited, such as night scenes, weather affected roads, and high speed highways. In summary, we make the following contributions:

- **First few-shot approach for attention-based generation.** We are **the first of its kind** to achieve joint spatial attention prediction and natural language explanation in a few-shot learning regime, training from fewer than 100 examples, two orders of magnitude more data efficient than existing joint modeling approaches [8, 9].
- **Attention shift anticipation.** Instead of focusing on current attention, our model introduces a structured attention reasoning representation that captures scene context, current focus, anticipated shift and causal factors. This enables models to predict where attention will move next from single frames, capturing the forward-looking nature of human attention without requiring video input at inference.
- **Dual-pathway architecture for joint learning.** We design an architecture with separate pathways for caption generation and attention-language alignment that share visual representations, enabling task-specific specialization while maintaining consistency.
- **Strong empirical validation.** Despite training in few-shot regime, we achieve competitive gaze prediction and caption generation with strong zero-shot transfer across three standard benchmarks demonstrating generalization beyond the training data distribution.

2 Related Works

2.1 Driver Attention Modeling

Driver attention modeling has been studied as a visual saliency prediction task, estimating spatial gaze heatmaps from dashcam images or video sequences [8]. Early works applied CNNs to learn correlations between scene features and eye fixations, while subsequent models incorporated temporal dynamics and multi-modal inputs using CNN-LSTMs and feature fusion from RGB, optical flow, and semantic segmentation [13, 10]. The SEEV model [14] outlines bottom-up (salience, effort) and top-down (expectancy, value) factors influencing attention allocation. Existing models

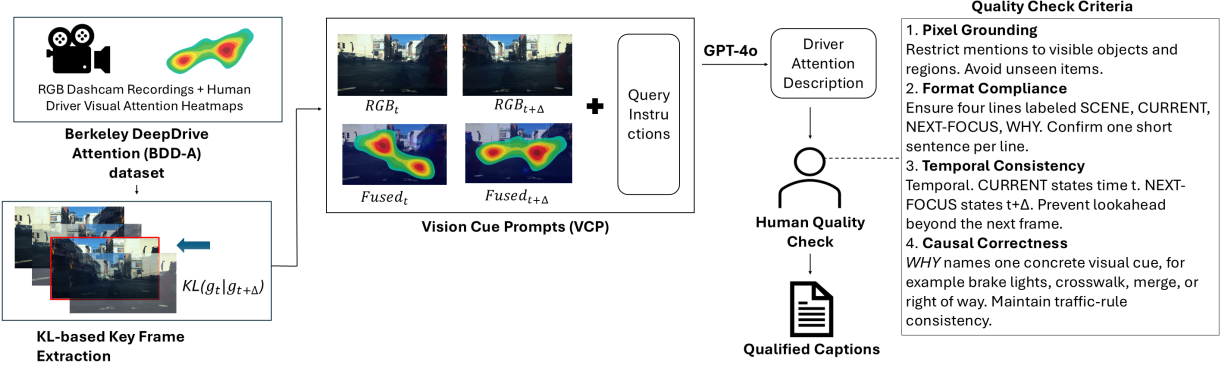


Figure 2: Dataset curation pipeline. From BDD-A [10] videos to paired frames, GPT-4o captioning with fixed template, human verification, and final captions. Full details in Appendix.

typically emphasize either low-level visual features or task-level signals such as GPS and traffic semantics [15, 2]. These approaches provide limited insights into the underlying causes of attention allocation beyond saliency.

2.2 Vision-Language Models for Explainable Attention

Recent work has applied VLMs to enhance attention interpretability through natural language. “Attention Neural Baby Talk” [16] generates captions highlighting hazardous elements by aligning attention masks with descriptions, while DRAMA [17] pairs videos with QA annotations explaining risk rationale. Large-scale VLMs like BLIP [18], Flamingo [19], and LLaVA [20] have enabled new approaches through vision-language pretraining and few-shot learning capabilities [21, 22, 23].

For driver attention specifically, LLada [8] proposes joint modeling of attention maps and textual descriptions through their W3DA dataset (70k samples), predicting both where drivers look and why attention is allocated. GazeXplain [9] generates natural language descriptions of gaze scanpaths for general visual attention.

2.3 Few-Shot Learning and Data-Efficient Adaptation

Few-shot learning addresses generalization from minimal examples. In semantic segmentation, PANet [24] achieves 48.1% mIoU with 5 images per class, while few-shot object detection methods report 15-30% AP with 10-30 examples [25, 26, 27]. In generative modeling, DreamBooth [28] personalizes Stable Diffusion using 3-5 images (CLIP-1 0.74), while UFC [29] achieves 87.3% accuracy with 30 examples versus 89.1% for fully-supervised baselines (10K+ examples).

Parameter-efficient fine-tuning enables adaptation with minimal updates. LoRA [30] matches full fine-tuning performance while updating 0.01% of parameters, reducing GPT-3’s trainable parameters from 175B to 4.7M. For VLMs, LoRA adaptation maintains 95%+ performance with 10-20M trainable parameters [31]. Flamingo demonstrates in-context learning, improving VQAv2 from 49.2% (0-shot) to 63.1% (32-shot) [19], though this approach shows high variance and struggles with structured outputs like spatial maps [32].

In autonomous driving, few-shot learning remains underexplored. Most attention systems train on hundreds of thousands of frames [11, 33, 34].

3 Method

We present our few-samples dependent driver attention modeling framework that joints modeling of spatial driver attention prediction and structured natural language explanation. These two tasks depend on totally different kinds of spatial understanding, where captioning needs global semantic reasoning while gaze prediction requires localized spatial sensitivity. A shared cross-attention module tends to overfit one task and underfit another [35, 36]. To address this imbalance, we introduce a dual-pathway architecture (Figure 3) in which gaze prediction and caption generation are handled by separate modules while still leveraging shared visual features. A vision-language alignment mechanism further provides semantic supervision to spatial prediction, ensuring predicted attention regions correspond to meaningful visual content. This design enables effective joint learning despite data scarcity.

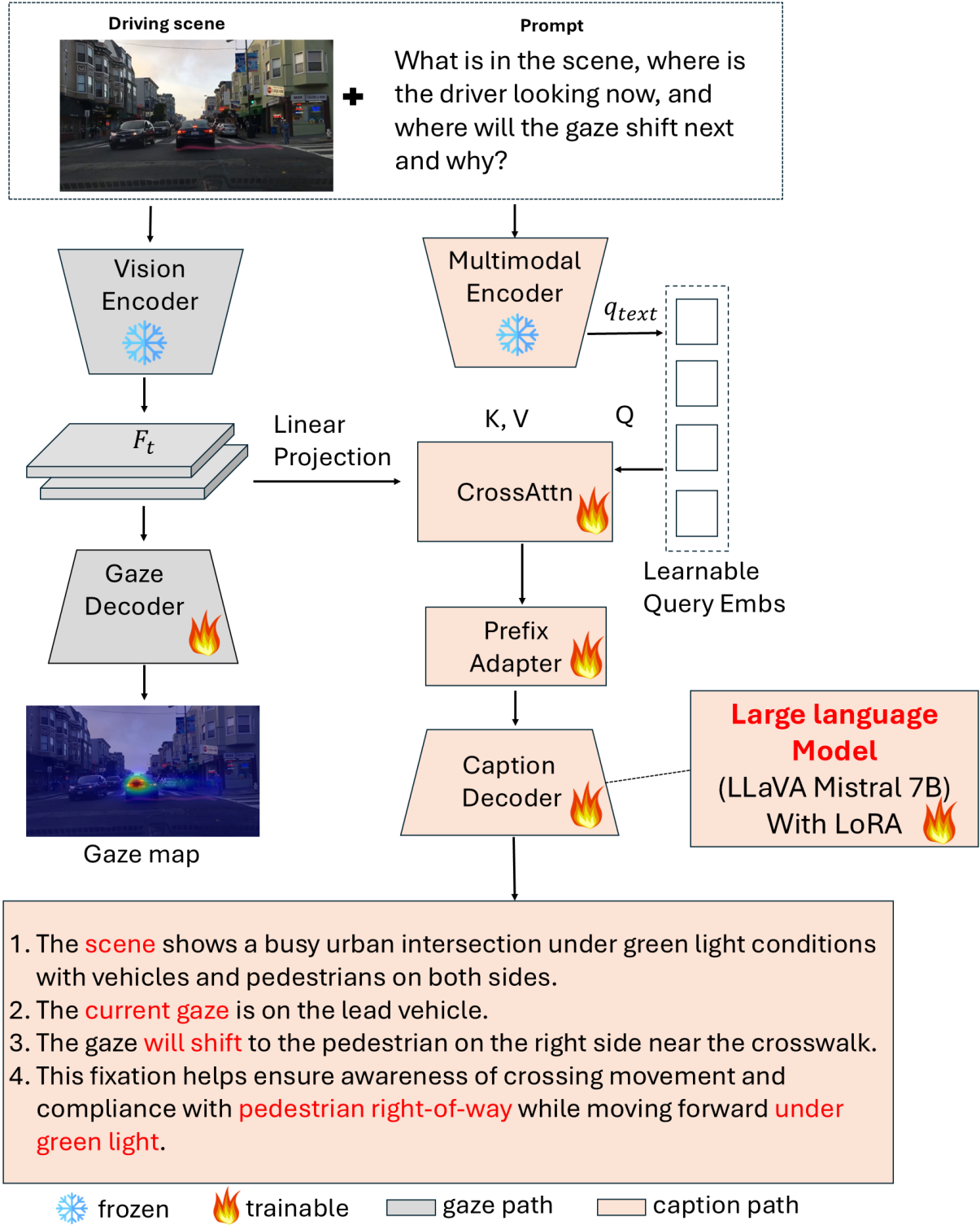


Figure 3: FSDAM architecture for joint gaze prediction and caption generation. A frozen vision-language backbone extracts spatial features F_t and text embeddings q_{text} . The gaze pathway, left, upsamples F_t to predict attention and gaze maps \hat{G} . The caption pathway, right, uses cross-attention over F_t to generate structured explanations.

3.1 Problem Formulation

Given a driving scene image $I \in \mathbb{R}^{H \times W \times 3}$, we jointly predict: (1) a spatial attention distribution $\hat{G} \in \Delta^{S \times S}$ indicating where the driver looks, where $\Delta^{S \times S}$ denotes the probability simplex over an $S \times S$ grid with $S=64$, and (2) a structured attention reasoning representation \hat{y} following the format:

$$\hat{y} = (C_{\text{scene}}, C_{\text{current}}, C_{\text{next}}, C_{\text{why}}) \quad (1)$$

Here, C_{scene} summarizes the global scene context, C_{current} describes the driver's present focus of attention, C_{next} anticipates how the attention is likely to shift next ("will check the crosswalk"), and C_{why} provides the causal rationale underlying this transition. Together, the four components form a structured attention reasoning representation that links spatial attention patterns with high-level semantic explanations, enabling the model to learn gaze behavior from single frames.

Our architecture builds upon LLaVA-Next-1.6 [37], which comprises a CLIP-ViT-L/14 vision encoder [6] extracting spatial features $F_t \in \mathbb{R}^{B \times 1024 \times 24 \times 24}$ and a Mistral-7B language model [38] producing image-conditioned text embeddings $q_{\text{text}} \in \mathbb{R}^{B \times d_e}$ through multimodal fusion [19, 37]. These frozen features feed into specialized pathways for gaze prediction and caption generation, with task-specific adaptation enabled by LoRA [30]. We optimize 13.6M task-specific parameters (0.2% of the 7B backbone) while keeping pretrained components frozen to prevent overfitting.

3.2 Spatial Attention Prediction

The gaze pathway predicts where drivers look. A convolutional decoder upsamples F_t from 24×24 to 64×64 resolution through successive convolution and bilinear upsampling layers [39, 40], then applies spatial softmax to produce $\hat{G} \in \Delta^{S \times S}$.

We supervise with forward KL divergence to encourage covering all human fixation regions:

$$\mathcal{L}_{\text{KL}} = \text{KL}(G \parallel \hat{G}) = \sum_{i,j} G(i,j) \log \frac{G(i,j)}{\hat{G}(i,j)}. \quad (2)$$

This alone produces overly diffuse predictions under limited data. We augment with a blur-gap regularizer that applies Gaussian smoothing ($\sigma=1.0$) to \hat{G} to obtain \tilde{G} , then penalizes cases where blurring doesn't degrade prediction:

$$\mathcal{L}_{\text{gaze}} = \mathcal{L}_{\text{KL}} + \lambda \cdot \max(0, \text{KL}(G \parallel \tilde{G}) - \mathcal{L}_{\text{KL}} + \epsilon), \quad (3)$$

with $\lambda=0.3$ and $\epsilon=0.05$. This encourages confident spatial localization in low-data regimes [41, 42]. The gaze pathway receives gradients only from $\mathcal{L}_{\text{gaze}}$ during forward passes, with semantic supervision added through alignment (Section 3.4).

3.3 Attention-Grounded Caption Generation

Following prefix-tuning [43], we expand q_{text} into M queries via projection W_{cap} , then perform cross-attention [44] over F_t :

$$Q = W_{\text{cap}}(q_{\text{text}}) \in \mathbb{R}^{B \times M \times d}, \quad \text{CTX} = \text{CrossAttn}(Q, K, V). \quad (4)$$

Mean pooling aggregates M context vectors into \bar{c}_{cap} , which a Prefix Adapter Ψ projects to visual prefix tokens $P = \Psi(\bar{c}_{\text{cap}})$ conditioning the decoder. We supervise with autoregressive cross-entropy:

$$\mathcal{L}_{\text{cap}} = - \sum_{t=1}^T \log p_{\theta}(y_t \mid y_{<t}, P, I), \quad (5)$$

where y contains scene description, current attention, anticipated shift, and causal reasoning. LoRA [30] enables task-specific tuning while keeping most parameters frozen.

3.4 Vision-Language Alignment

To ensure predicted attention regions align with semantic content, we introduce a training-only alignment mechanism. A dedicated cross-attention block processes text queries q_{text} to produce text-conditioned features \bar{c}_{gaze} . In parallel, we pool spatial features F_t using predicted gaze \hat{G}_{\downarrow} (downsampled to match F_t resolution) as soft weights:

$$z_{\text{vis}} = \sum_{i,j} \hat{G}_{\downarrow}(i,j) F_t[:, :, i, j]. \quad (6)$$

using the model’s own prediction maintains consistency between training and inference [45, 46].

Both representations project into a shared 256-dimensional space via learned projections P_{vis} and P_{txt} , producing $u^{\text{vis}} = P_{\text{vis}}(z_{\text{vis}})$ and $u^{\text{txt}} = P_{\text{txt}}(\bar{c}_{\text{gaze}})$. We align these with InfoNCE contrastive loss [47]:

$$\mathcal{L}_{\text{align}} = -\frac{1}{B} \sum_{i=1}^B \log \frac{\exp(\text{sim}(u_i^{\text{vis}}, u_i^{\text{txt}})/\tau)}{\sum_{j=1}^B \exp(\text{sim}(u_i^{\text{vis}}, u_j^{\text{txt}})/\tau)}, \quad (7)$$

where $\text{sim}(\cdot, \cdot)$ denotes cosine similarity and τ is a temperature parameter. Gradients pass through spatial pooling to the gaze decoder, pushing attention toward semantically relevant regions.

3.5 Training and Inference

We jointly optimize all three objectives through a weighted combination:

$$\mathcal{L} = w_g \mathcal{L}_{\text{gaze}} + w_c \mathcal{L}_{\text{cap}} + w_a \mathcal{L}_{\text{align}}, \quad (8)$$

where $(w_g, w_c, w_a) = (1.0, 1.0, 0.2)$ balance gaze prediction, caption generation, and vision-language alignment. The weights were chosen through a small-scale grid search on a validation split and were stable across experiments.

Training. We train using AdamW optimizer with separate learning rates for LoRA and task modules. Training uses mixed precision, gradient accumulation for an effective batch of 16, and input size 336×336 . Only LoRA and lightweight adapters are updated, totaling 13.6M trainable parameters ($\sim 0.2\%$ of the backbone). Learning rate is adjusted via a ReduceLROnPlateau scheduler.

Inference. During inference, only gaze and caption branches are active. The gaze decoder predicts \hat{G} from visual features F_t , while the caption pathway generates structured explanations through cross-attention and prefix adaptation. The alignment module is used only during training and adds no cost at inference.

4 Experimental Setup

Dataset Preparation. We construct a gaze-language dataset from BDD-A dataset [10], which contains braking event videos selected from large-scale, crowd-sourced driving video data combined with compiled human gaze data from 6.5 seconds prior and 3.5 seconds after each braking event. To identify frames capturing meaningful attention transitions, we employ a KL-divergence-based selection algorithm [48] that detects moments of maximum gaze distribution change between consecutive frames. Local peaks in the KL divergence curve mark anchor frames t where attention shifts abruptly. For each anchor, we select a target frame $t + \Delta$ within $[3, 18]$ frames that maximizes divergence from the anchor, capturing the strongest future attention transition. Following temporal sampling strategies from video action recognition [49], we filter clips shorter than 50 frames and retain the top - $K = 2$ anchor-target pairs per video for temporal diversity. Each resulting sample $(I_t, I_{t+\Delta}, G_t, G_{t+\Delta})$ consists of two frames and their corresponding gaze maps. We generate structured captions via GPT-4o [50] with human verification (Figure 2), producing 90 training examples across eight diverse driving scenarios.

Implementation Details. All experiments are implemented in PyTorch [51]. We build on the LLaVA-Next Mistral-7B backbone, which integrates a CLIP-based vision tower pretrained on large-scale image–text pairs. The vision–language backbone remains frozen during training, and only lightweight task-specific components (gaze decoder, prefix adapter, alignment head, and LoRA adapters) are updated. Training is performed on a single NVIDIA GH200 GPU with input resolution 336×336 , batch size 4, and gradient accumulation over 4 steps (effective batch 16). We use the AdamW optimizer with learning rates of 1×10^{-4} for LoRA and 2×10^{-4} for task heads, a ReduceLROnPlateau scheduler (factor 0.5, patience 2), and mixed precision of bfloat16.

Evaluation Metrics We evaluate our model using standard saliency and captioning metrics. For gaze prediction, we adopt CC, KL, SIM, AUC-J, AUC-B, and NSS following the official MIT Saliency Benchmark [52]. For caption generation, we report BLEU, METEOR, ROUGE-L, CIDEr-R, and BERTScore using the COCO Caption Evaluation Toolkit [53]. All metrics are computed using their standardized implementations to ensure fair comparison with prior work.

5 Results & Analysis

5.1 Baselines

We evaluate FSDAM on four driver attention datasets: BDD-A [10], DADA-2000 [12], DReyeVE [11], and W3D [8], comparing against seven baselines: U²-Net [54], MINet [55], DBNet [56], DeepLabV3 [57], and LLada [8]. These models represent current approaches in saliency and driver attention research. All baselines were trained on the complete BDD-A training set and tested on each dataset’s official test split. For LLada [8], we report published results LLada was trained on the W3D dataset.

For caption prediction, we evaluate FSDAM on the W3D benchmark and compare it with models representing the current spectrum of driver attention approaches, from fully supervised to zero-shot and few-shot methods. Fully trained baselines including GazeXplain [9] and LLada [8] utilize the complete W3D [8] training dataset (70k samples). Zero-shot and in-context models such as Qwen-VL [58] and LLaVA [20] are evaluated without task-specific fine-tuning, with Qwen-VL [58] using in-context learning via fine-tuning prompts. Few-shot baselines combine gaze prediction models with language models—DeepGazeIIE [59] + LLaVA [20] and MLNet [60] + LLaVA [20] employ a two-stage approach where gaze heatmaps are first generated then fed to the language model, both trained on the same 90 BDD-A samples as our method. FSDAM (Ours) uses an end-to-end architecture trained on 90 BDD-A samples and is evaluated on the W3D test set across three driving scenarios: normal driving, safety-critical situations, and traffic accidents, demonstrating the effectiveness of our unified gaze-language approach against both data-rich and data-efficient alternatives.

5.2 Quantitative Analysis

5.2.1 Spatial Attention Prediction

Table 1 reports quantitative results for driver attention prediction across four datasets. All reproduced models were trained on BDD-A for consistency. FSDAM provides a strong balance between sample efficiency and predictive accuracy. With only 90 training samples, it reaches performance that aligns with or exceeds models trained on much larger datasets, including W3D with \sim 70K frames, DADA-2000 with 658K frames, and DR(eye)VE with 555K frames.

On BDD-A[11], FSDAM obtains the lowest KL divergence at 1.13. This improves over LLada[8] by 2.6% and over DBNet[56] by 13%. It matches LLada[8] in CC at 0.60 and ranks second in NSS at 4.10, indicating better spatial attention prediction. Compared to the fully supervised MINet[55], FSDAM improves CC by 30% and reduces KL divergence by 89%, which highlights its effectiveness with limited data.

Our cross-dataset evaluation demonstrates the strong transferability of our approach. On DR(eye)VE[11], FSDAM reaches the lowest KL divergence at 0.77, improving over LLada[8] by 26% and DBNet[56] by 57%. It also achieves the highest SIM at 0.54, a 20% gain over U²-Net[54]. This shows that vision language alignment helps capture domain stable attention cues that transfer to highway scenarios.

On DADA-2000[12], FSDAM maintains competitive performance while using far fewer samples, achieving the best KL divergence at 1.64 with a 10% gain over LLada[8] and a 13% gain over DBNet[56]. On W3D, FSDAM matches DeepLabV3[57] in CC at 0.53 and beats LLada in KL divergence at 1.27 by 13%. It also achieves the second best SIM at 0.44 and NSS at 3.50.

These results show that extensive supervision is not required for strong driver attention modeling. FSDAM ranks first in KL divergence on three of the four datasets with an average 15% margin over the next best method. This establishes the proposed few shot vision language framework as a practical and scalable solution for new driving domains where large gaze annotation sets are not available.

Table 1: Quantitative comparison of driver attention prediction across four datasets. All reproduced models were trained on BDD-A dataset. **Bold** indicates best performance, underlined indicates second best. * denotes results reported from original papers.

Method	BDD-A					DADA-2000					DR(eye)VE					W3D								
	CC \uparrow	KL \downarrow	SIM \uparrow	AUC-J \uparrow	AUC-B \uparrow	NSS \uparrow	CC \uparrow	KL \downarrow	SIM \uparrow	AUC-B \uparrow	NSS \uparrow	CC \uparrow	KL \downarrow	SIM \uparrow	AUC-B \uparrow	NSS \uparrow	CC \uparrow	KL \downarrow	SIM \uparrow	AUC-J \uparrow	AUC-B \uparrow	NSS \uparrow		
U ² -Net [54]	0.56	1.50	0.47	0.94	<u>0.88</u>	3.95	0.42	2.18	0.37	0.91	0.82	2.73	0.57	1.52	0.45	0.90	0.82	3.20	0.44	2.10	<u>0.37</u>	0.90	0.81	2.81
MINet [55]	0.46	10.3	0.16	0.89	<u>0.82</u>	3.67	0.32	10.45	0.14	0.82	0.73	2.02	0.44	8.87	0.36	0.84	0.80	2.65	0.35	10.51	0.14	0.83	0.77	2.54
DBNet [56]	<u>0.57</u>	1.30	0.41	0.95	0.91	4.41	0.41	1.89	0.29	<u>0.93</u>	<u>0.85</u>	3.08	0.48	1.79	0.29	0.91	0.85	<u>3.71</u>	0.47	1.77	0.33	0.93	0.86	3.50
DeepLabV3 [57]	0.47	9.62	0.21	0.97	0.75	2.56	0.42	10.26	0.19	0.96	0.73	2.23	0.67	8.78	0.47	0.91	0.84	2.74	0.53	9.70	0.32	0.93	0.81	2.35
LLada* [8]	0.60	<u>1.16</u>	0.47	—	—	0.48	<u>1.82</u>	<u>0.36</u>	—	—	0.67	<u>1.04</u>	—	—	—	—	<u>0.52</u>	<u>1.46</u>	<u>0.37</u>	0.95	0.90	4.62		
FSDAM (Ours)	0.60	1.13	<u>0.43</u>	0.96	0.91	<u>4.10</u>	<u>0.44</u>	1.64	0.33	0.92	0.86	<u>2.95</u>	<u>0.61</u>	<u>0.77</u>	0.54	0.91	<u>0.84</u>	4.04	0.53	1.27	0.44	<u>0.91</u>	0.87	3.50

Table 2: Comparison of captioning performance across driving scenarios on W3D dataset. Fully-trained baselines use the original W3D training data, Zero-shot and ICL models require no fine-tuning, and our FSDAM and few-shot baselines are trained on a 90-sample BDD-A subset. Higher is better.

Method	Training Regime	Normal Driving				Safety-Critical Situation				Traffic Accident			
		BLEU	METEOR	ROUGE	CIDEr-R	BLEU	METEOR	ROUGE	CIDEr-R	BLEU	METEOR	ROUGE	CIDEr-R
<i>Fully Trained on W3D</i>													
GazeXplain* [9]	Full-data (W3D) [~70k samples]	0.31	0.30	0.22	0.42	0.19	0.29	0.37	0.55	0.17	0.20	0.44	0.66
LLada [†] [8]	Full-data (W3D) [~70k samples]	0.44	<u>0.36</u>	0.58	<u>0.96</u>	0.44	0.38	0.59	<u>1.23</u>	<u>0.38</u>	<u>0.32</u>	0.52	1.00
<i>Zero-shot and In-Context Models</i>													
Owen-VL [58]	Zero-shot (no training)	0.10	0.19	0.28	0.34	0.19	0.21	0.29	0.13	0.08	0.21	0.29	0.12
LLaVA [20]	Zero-shot (no training)	0.12	0.14	0.23	0.35	0.13	0.19	0.11	0.10	0.17	0.26	0.19	0.13
Owen-VL [58]	In-context learning (no fine-tuning)	0.13	0.18	0.22	0.36	0.21	0.17	0.30	0.23	0.12	0.24	0.33	0.15
<i>Few-shot Learning (BDD-A 90 samples)</i>													
DeepGazeI[61] + LLaVA	Few-shot	0.12	0.23	0.28	0.14	0.13	0.22	0.30	0.18	0.15	0.21	0.31	0.17
DeepGazeIIE[59] + LLaVA	Few-shot	0.11	0.18	0.26	0.17	0.11	0.20	0.32	0.13	0.11	0.19	0.34	0.10
MLNet[60] + LLaVA	Few-shot	0.13	0.19	0.27	0.31	0.26	0.20	0.32	0.12	0.13	0.18	0.33	0.28
FSDAM (Ours)	Few-shot	<u>0.42</u>	0.37	<u>0.48</u>	<u>0.83</u>	<u>0.35</u>	<u>0.33</u>	<u>0.46</u>	0.47	<u>0.33</u>	0.35	0.34	<u>0.84</u>

5.2.2 Caption Prediction Analysis

Table 2 presents caption generation performance across three driving categories on the W3D dataset. Despite using only 90 training samples from BDD-A, our FSDAM achieves remarkable results that rival or exceed fully-trained baselines using the complete W3D dataset. In normal driving scenarios, FSDAM attains strong performance (BLEU: 0.42, METEOR: 0.37, CIDEr-R: 0.83) competitive with LLada (BLEU: 0.44, METEOR: 0.36, CIDEr-R: 0.96), which is trained on the full dataset. Notably, FSDAM demonstrates robust generalization to challenging scenarios, achieving competitive scores in safety-critical situations (BLEU: 0.35, METEOR: 0.33) and traffic accidents (BLEU: 0.33, METEOR: 0.35, CIDEr-R: 0.84). Compared to other few-shot baselines combining existing gaze models with LLaVA, FSDAM shows substantial improvements—achieving up to 3.2 times higher BLEU scores (0.42 vs. 0.13 for MLNet[55]+LLaVA in normal driving). Zero-shot approaches yield limited performance (BLEU < 0.21), underscoring the value of our few-shot learning framework, which effectively bridges the gap between zero-shot and full-data training regimes while preserving high performance efficiency.

5.3 Qualitative Results

Figure 4 presents qualitative comparisons against fully-supervised baselines U2-Net [54] and DeepLabV3 [57]. Row (a) demonstrates peripheral hazard detection where FSDAM produces a broader attention distribution extending toward the right-side pedestrian area, while baselines concentrate more tightly on the stop sign region. In the complex intersection scenario (row c) with multiple pedestrians and vehicles, FSDAM generates the most spatially extensive attention coverage across agents, while U2-Net produces more concentrated predictions and DeepLabV3 [57] exhibits multiple distinct hot spots, potentially missing critical areas. Row (e) illustrates left-turn navigation where FSDAM effectively captures distributed attention spanning both the lead vehicle and the turning trajectory, demonstrating the benefit of vision-language alignment in understanding maneuver semantics, while baselines show more localized attention patterns. Row (d) shows all methods successfully localizing attention to the lane-changing vehicle’s brake light area, with comparable spatial precision across approaches.

Row (b) presents a challenging scenario where ground truth exhibits distributed attention across both the lead vehicle and a right-side pedestrian. All methods concentrate primarily on the vehicle, missing the distributed pattern. Despite this shared challenge, FSDAM demonstrates strong performance across diverse driving scenarios, producing attention predictions with superior spatial coverage in multi-agent situations (rows a, c, e) and comparable precision in focused attention tasks (row d). These results validate that our vision-language alignment approach enables effective few-shot learning, achieving spatial and semantic coherence competitive with fully-supervised methods trained on substantially larger datasets.

5.4 Few-Shot Learning Analysis

Figure 1 presents the impact of varying support set sizes on gaze prediction performance across six metrics. FSDAM demonstrates efficient learning dynamics, with substantial improvements from 1-shot to 5-shot settings. Performance gains are most pronounced between 1-shot and 3-shot (e.g., NSS increases from 2.32 to 3.64, CC improves from 0.41 to 0.53), after which the improvements plateau. Notably, our 5-shot model achieves performance (CC: 0.58, SIM: 0.43, NSS: 4.09, KL: 1.17) that closely approaches the full-data baseline (CC: 0.60, SIM: 0.43, NSS: 4.10, KL: 1.13), recovering 96.7% of full-data CC performance and 99.8% of NSS performance with only five support samples. The KL divergence shows consistent reduction from 1.74 to 1.17 as support size increases, indicating improved distribution

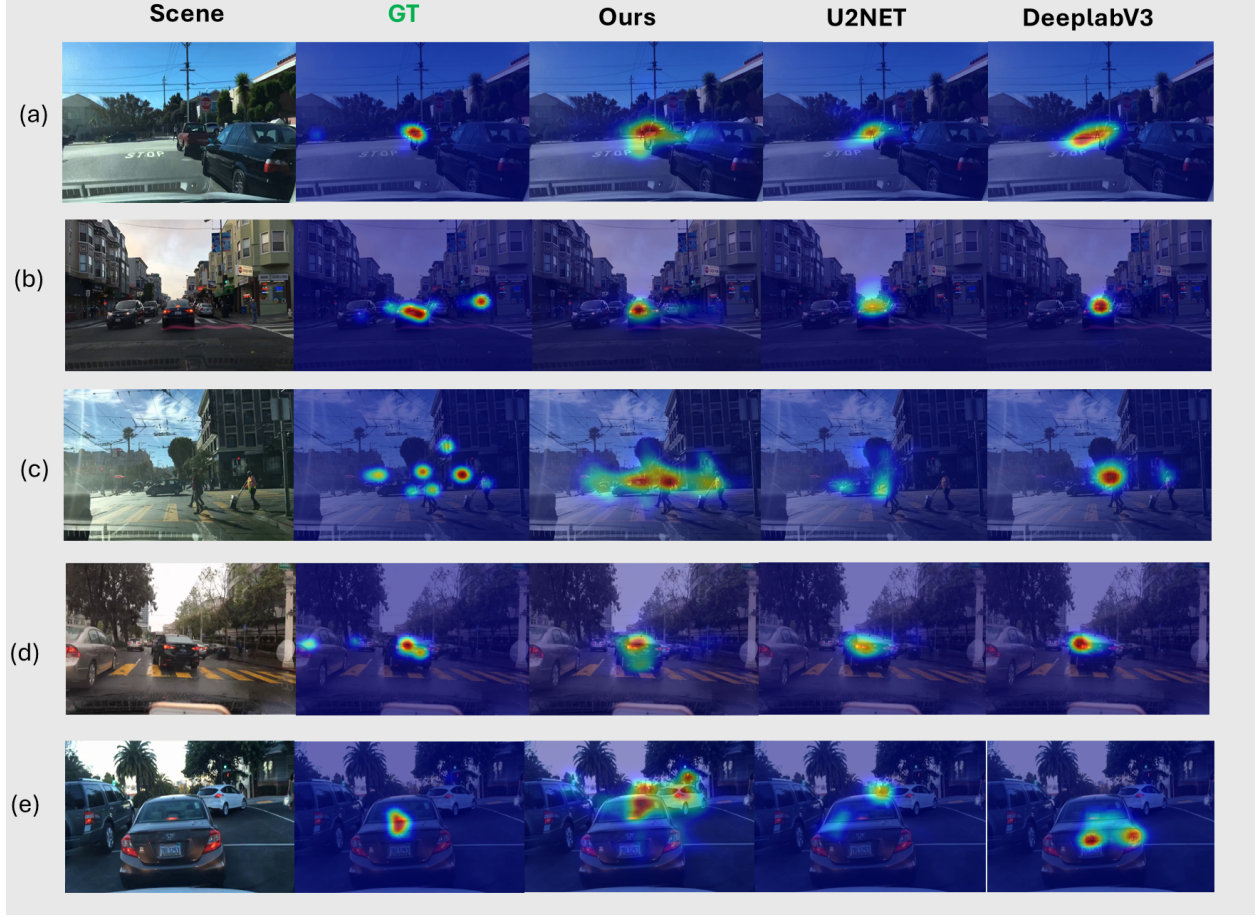


Figure 4: Qualitative comparison of driver attention prediction on BDD-A test scenes showing the input image and attention heatmaps from ground truth, FSDAM trained on 90 samples, U2-Net[54], and DeepLabV3[57].

matching. This analysis validates FSDAM’s data efficiency: meaningful gaze predictions emerge from minimal supervision, with performance rapidly saturating after 3-5 examples, making our approach practical for real-world deployment where annotated driver attention data is scarce.

5.5 Ablations

We conduct systematic ablation experiments to assess each component’s contribution in FSDAM. For gaze prediction, we evaluate on the official BDD-A test set. For caption generation, we evaluate on 49 curated samples with structured explanations. We compare four variants: **Gaze-Only** trains only gaze prediction; **Caption-Only** trains only caption generation; **Shared Cross-Attention** uses a single cross-attention module for both tasks; and **Full FSDAM** uses task-specific cross-attention modules with vision–language alignment.

Figure 6 shows a consistent performance hierarchy across both tasks. The shared cross-attention variant provides marginal gains over single-task baselines but degrades gaze prediction (4% higher KL divergence), indicating negative transfer. In contrast, full FSDAM achieves substantial improvements: **31.9% KL reduction**, **43.3% SIM improvement**, and **66.7% NSS improvement** for gaze prediction, alongside **32.4% ROUGE-L**, **7.1% CIDEr-R**, and **3.4% BERTScore improvements** for caption generation, all relative to single-task baselines. This hierarchy (single-task < shared < dual-pathway) validates three design principles: joint training enables mutual benefits through shared visual representations, task-specific cross-attention modules prevent negative transfer, and dual pathways with vision–language alignment enable effective few-shot learning.

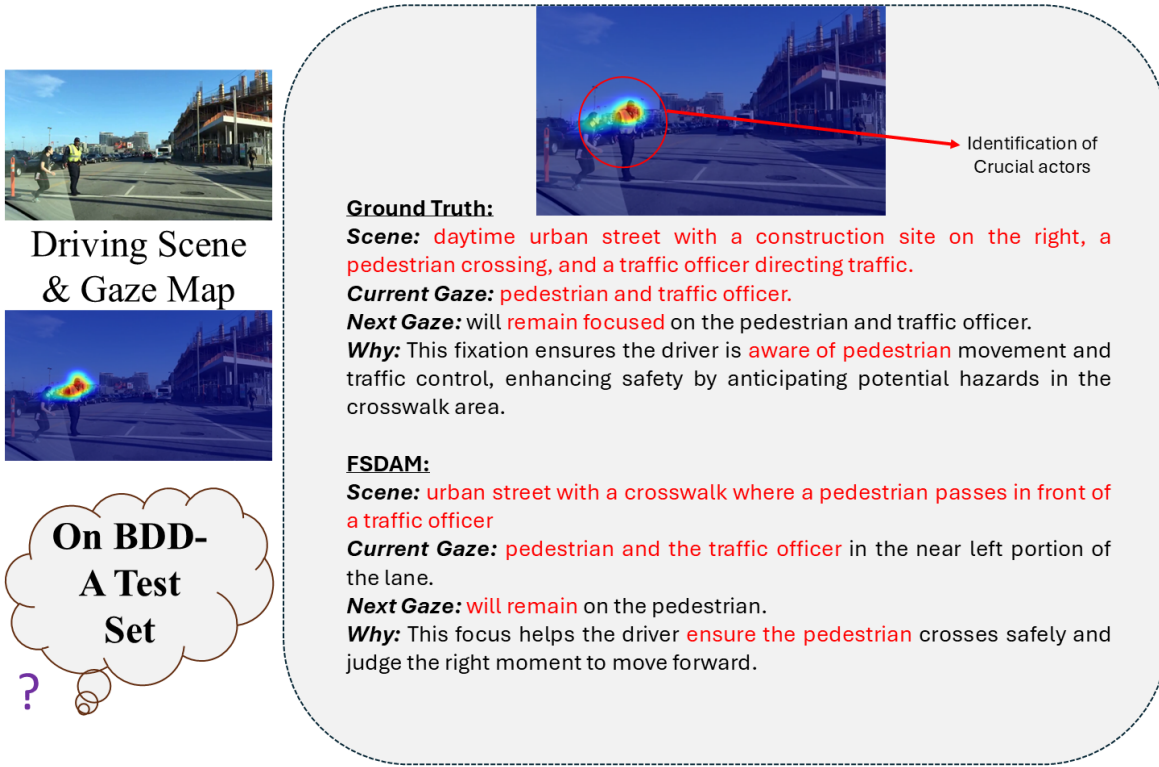


Figure 5: Driving scene and model output showing the input frame, its ground truth gaze map, and the corresponding FSDAM prediction. The model produces attention heatmaps over key regions and generates structured attention reasoning.

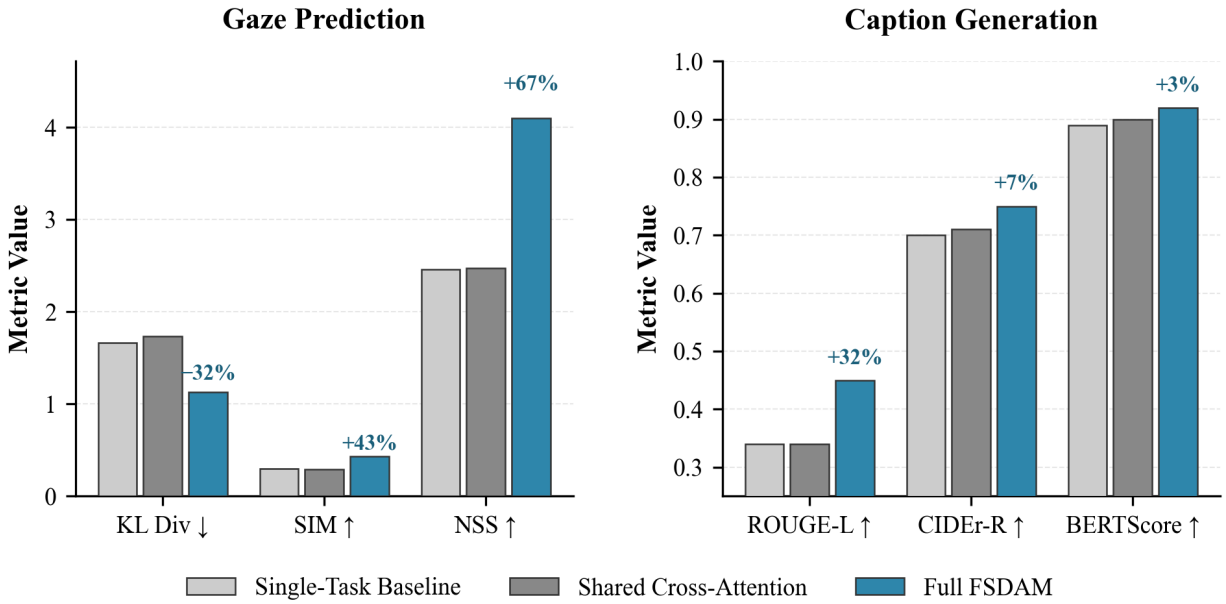


Figure 6: Ablation study comparing four architectural variants. The dual-pathway configuration in FSDAM achieves the largest percentage gains for both gaze prediction and caption generation.

6 Conclusions

We present FSDAM, a framework that achieves joint gaze prediction and natural language explanation from approximately 100 training examples. Through a dual-pathway architecture with vision-language alignment, we demonstrate competitive performance compared to fully-supervised methods, while introducing attention shift prediction. This paradigm also enables future implementation of a coupled sequential analysis framework, where forward predictions can be fed back into the system as guidance, functioning as policies or recommendations for performance adjustments. Our results validated this approach across multiple benchmarks (BDD-A, DR(eye)VE, DADA-2000, W3D), showing strong zero-shot generalization despite minimal supervision. The model generates contextually appropriate explanations across diverse driving scenarios, from normal conditions to safety-critical situations and accidents. This work demonstrated the feasibility of effective explainable attention modeling with manageable labeling. Our few-shot paradigm can facilitate practical deployment of visual attention prediction models in specialized domains where large-scale annotation may be infeasible. Future directions include temporal modeling through video inputs and explicit handling of distributed attention patterns to further improve anticipation accuracy in dynamic scenarios.

References

- [1] Jianwu Fang, Dingxin Yan, Jiahuan Qiao, Jianru Xue, and Hongkai Yu. Dada: Driver attention prediction in driving accident scenarios. *IEEE Transactions on Intelligent Transportation Systems*, 23(6):4959–4971, 2022.
- [2] Iuliia Kotseruba and John K. Tsotsos. Scout+: Towards practical task-driven drivers’ gaze prediction. In *2024 IEEE Intelligent Vehicles Symposium (IV)*, pages 1927–1932, 2024.
- [3] Yongkang Li, Kaixin Xiong, Xiangyu Guo, Fang Li, Sixu Yan, Gangwei Xu, Lijun Zhou, Long Chen, Haiyang Sun, Bing Wang, et al. Recogdrive: A reinforced cognitive framework for end-to-end autonomous driving. *arXiv preprint arXiv:2506.08052*, 2025.
- [4] Jacob Leon Kröger, Otto Hans-Martin Lutz, and Florian Müller. *What Does Your Gaze Reveal About You? On the Privacy Implications of Eye Tracking*, pages 226–241. Springer International Publishing, Cham, 2020.
- [5] Anurag Ghosh, Shen Zheng, Robert Tamburo, Khiem Vuong, Juan Alvarez-Padilla, Hailiang Zhu, Michael Cardei, Nicholas Dunn, Christoph Mertz, and Srinivasa G Narasimhan. Roadwork: A dataset and benchmark for learning to recognize, observe, analyze and drive through work zones. In *ICCV*, 2025.
- [6] Alec Radford, Jong Wook Kim, Chris Hallacy, Aditya Ramesh, Gabriel Goh, Sandhini Agarwal, Girish Sastry, Amanda Askell, Pamela Mishkin, Jack Clark, Gretchen Krueger, and Ilya Sutskever. Learning transferable visual models from natural language supervision, 2021.
- [7] Chonghao Sima, Katrin Renz, Kashyap Chitta, Li Chen, Hanxue Zhang, Chengen Xie, Jens Beißenwenger, Ping Luo, Andreas Geiger, and Hongyang Li. Drivelm: Driving with graph visual question answering, 2023.
- [8] Yuchen Zhou, Jiayu Tang, Xiaoyan Xiao, Yueyao Lin, Linkai Liu, Zipeng Guo, Hao Fei, Xiaobo Xia, and Chao Gou. Where, what, why: Towards explainable driver attention prediction. In *Proceedings of the IEEE/CVF International Conference on Computer Vision (ICCV)*, 2025.
- [9] Xianyu Chen, Ming Jiang, and Qi Zhao. Gazexplain: Learning to predict natural language explanations of visual scanpaths, 2024.
- [10] Ye Xia, Danqing Zhang, Jinkyu Kim, Ken Nakayama, Karl Zipser, and David Whitney. Predicting driver attention in critical situations. In C.V. Jawahar, Hongdong Li, Greg Mori, and Konrad Schindler, editors, *Computer Vision – ACCV 2018*, pages 658–674, Cham, 2019. Springer International Publishing.
- [11] Andrea Palazzi, Davide Abati, Francesco Solera, and Rita Cucchiara. Predicting the driver’s focus of attention: the dr (eye) ve project. *IEEE transactions on pattern analysis and machine intelligence*, 41(7):1720–1733, 2018.
- [12] Jianwu Fang, Dingxin Yan, Jiahuan Qiao, Jianru Xue, and Hongkai Yu. Dada: Driver attention prediction in driving accident scenarios, 2023.
- [13] Stefano Alletto, Andrea Palazzi, Francesco Solera, Simone Calderara, and Rita Cucchiara. Dr(eye)ve: A dataset for attention-based tasks with applications to autonomous and assisted driving. In *2016 IEEE Conference on Computer Vision and Pattern Recognition Workshops (CVPRW)*, pages 54–60, 2016.
- [14] Kelly S Steelman, Jason S McCarley, and Christopher D Wickens. Theory-based models of attention in visual workspaces. *International Journal of Human–Computer Interaction*, 33(1):35–43, 2017.
- [15] Lex Fridman, Daniel E. Brown, Michael Glazer, William Angell, Spencer Dodd, Benedikt Jenik, Jack Terwilliger, Aleksandr Patsekin, Julia Kindelsberger, Li Ding, Sean Seaman, Alea Mehler, Andrew Sipperley, Anthony

Pettinato, Bobbie D. Seppelt, Linda Angell, Bruce Mehler, and Bryan Reimer. Mit advanced vehicle technology study: Large-scale naturalistic driving study of driver behavior and interaction with automation. *IEEE Access*, 7:102021–102038, 2019.

[16] Yuki Mori, Hiroshi Fukui, Tsubasa Hirakawa, Jo Nishiyama, Takayoshi Yamashita, and Hironobu Fujiyoshi. Attention neural baby talk: Captioning of risk factors while driving. In *2019 IEEE Intelligent Transportation Systems Conference (ITSC)*, pages 4317–4322, 2019.

[17] Srikanth Malla, Chiho Choi, Isht Dwivedi, Joon Hee Choi, and Jiachen Li. Drama: Joint risk localization and captioning in driving. In *Proceedings of the IEEE/CVF Winter Conference on Applications of Computer Vision*, pages 1043–1052, 2023.

[18] Junnan Li, Dongxu Li, Caiming Xiong, and Steven Hoi. Blip: Bootstrapping language-image pre-training for unified vision-language understanding and generation. In *ICML*, 2022.

[19] Jean-Baptiste Alayrac, Jeff Donahue, Pauline Luc, Antoine Miech, Iain Barr, Yana Hasson, Karel Lenc, Arthur Mensch, Katie Millican, Malcolm Reynolds, Roman Ring, Eliza Rutherford, Serkan Cabi, Tengda Han, Zhitao Gong, Sina Samangooei, Marianne Monteiro, Jacob Menick, Sebastian Borgeaud, Andrew Brock, Aida Nematzadeh, Sahand Sharifzadeh, Mikolaj Binkowski, Ricardo Barreira, Oriol Vinyals, Andrew Zisserman, and Karen Simonyan. Flamingo: a visual language model for few-shot learning, 2022.

[20] Haotian Liu, Chunyuan Li, Qingyang Wu, and Yong Jae Lee. Visual instruction tuning. In *Proceedings of the 37th International Conference on Neural Information Processing Systems, NIPS '23*, Red Hook, NY, USA, 2023. Curran Associates Inc.

[21] Zhenhua Xu, Yujia Zhang, Enze Xie, Zhen Zhao, Yong Guo, Kwan-Yee. K. Wong, Zhengu Li, and Hengshuang Zhao. Drivegpt4: Interpretable end-to-end autonomous driving via large language model, 2024.

[22] Xiaoyu Tian, Junru Gu, Bailin Li, Yicheng Liu, Zhiyong Zhao, Yang Wang, Kun Zhan, Peng Jia, Xianpeng Lang, and Hang Zhao. Drivevlm: The convergence of autonomous driving and large vision-language models. *arXiv preprint arXiv:2402.12289*, 2024.

[23] Xingcheng Zhou, Mingyu Liu, Ekim Yurtsever, Bare Luka Zagar, Walter Zimmer, Hu Cao, and Alois C. Knoll. Vision language models in autonomous driving: A survey and outlook, 2024.

[24] Kaixin Wang, Jun Hao Liew, Yingtian Zou, Daquan Zhou, and Jiashi Feng. Panet: Few-shot image semantic segmentation with prototype alignment, 2020.

[25] Bingyi Kang, Zhuang Liu, Xin Wang, Fisher Yu, Jiashi Feng, and Trevor Darrell. Few-shot object detection via feature reweighting, 2019.

[26] Qi Fan, Wei Zhuo, Chi-Keung Tang, and Yu-Wing Tai. Few-shot object detection with attention-rpn and multi-relation detector, 2020.

[27] Zhenyu Yan, Qingqing Fang, Wenxi Lv, and Qinliang Su. Anomalsd: Few-shot multi-class anomaly detection with stable diffusion model, 2024.

[28] Nataniel Ruiz, Yuanzhen Li, Varun Jampani, Yael Pritch, Michael Rubinstein, and Kfir Aberman. Dreambooth: Fine tuning text-to-image diffusion models for subject-driven generation, 2023.

[29] Donggyun Kim, Jinwoo Kim, Seongwoong Cho, Chong Luo, and Seunghoon Hong. Universal few-shot learning of dense prediction tasks with visual token matching, 2023.

[30] Edward J Hu, Yelong Shen, Phillip Wallis, Zeyuan Allen-Zhu, Yuanzhi Li, Shean Wang, Lu Wang, and Weizhu Chen. LoRA: Low-rank adaptation of large language models. In *International Conference on Learning Representations*, 2022.

[31] Neil Houlsby, Andrei Giurgiu, Stanislaw Jastrzebski, Bruna Morrone, Quentin de Laroussilhe, Andrea Gesmundo, Mona Attariyan, and Sylvain Gelly. Parameter-efficient transfer learning for nlp, 2019.

[32] Qingxiu Dong, Lei Li, Damai Dai, Ce Zheng, Jingyuan Ma, Rui Li, Heming Xia, Jingjing Xu, Zhiyong Wu, Tianyu Liu, Baobao Chang, Xu Sun, Lei Li, and Zhifang Sui. A survey on in-context learning, 2024.

[33] Ye Xia, Danqing Zhang, Jinkyu Kim, Ken Nakayama, Karl Zipser, and David Whitney. Predicting driver attention in critical situations, 2018.

[34] Jianwu Fang, Dingxin Yan, Jiahuan Qiao, Jianru Xue, He Wang, and Sen Li. Dada-2000: Can driving accident be predicted by driver attention? analyzed by a benchmark, 2019.

[35] Dongyue Li, Aneesh Sharma, and Hongyang R. Zhang. Scalable multitask learning using gradient-based estimation of task affinity. In *Proceedings of the 30th ACM SIGKDD Conference on Knowledge Discovery and Data Mining, KDD '24*, page 1542–1553. ACM, August 2024.

[36] Christopher Fifty, Ehsan Amid, Zhe Zhao, Tianhe Yu, Rohan Anil, and Chelsea Finn. Efficiently identifying task groupings for multi-task learning, 2021.

[37] Haotian Liu, Chunyuan Li, Yuheng Li, Bo Li, Yuanhan Zhang, Sheng Shen, and Yong Jae Lee. Llava-next: Improved reasoning, ocr, and world knowledge, January 2024.

[38] Albert Q. Jiang, Alexandre Sablayrolles, Arthur Mensch, Chris Bamford, Devendra Singh Chaplot, Diego de las Casas, Florian Bressand, Gianna Lengyel, Guillaume Lample, Lucile Saulnier, Lélio Renard Lavaud, Marie-Anne Lachaux, Pierre Stock, Teven Le Scao, Thibaut Lavril, Thomas Wang, Timothée Lacroix, and William El Sayed. Mistral 7b, 2023.

[39] Jonathan Long, Evan Shelhamer, and Trevor Darrell. Fully convolutional networks for semantic segmentation, 2015.

[40] Olaf Ronneberger, Philipp Fischer, and Thomas Brox. U-net: Convolutional networks for biomedical image segmentation, 2015.

[41] Matthias Kümmerer, Thomas S. A. Wallis, and Matthias Bethge. Deepgaze ii: Reading fixations from deep features trained on object recognition, 2016.

[42] Marcella Cornia, Lorenzo Baraldi, Giuseppe Serra, and Rita Cucchiara. Predicting Human Eye Fixations via an LSTM-based Saliency Attentive Model. *IEEE Transactions on Image Processing*, 27(10):5142–5154, 2018.

[43] Xiang Lisa Li and Percy Liang. Prefix-tuning: Optimizing continuous prompts for generation, 2021.

[44] Ashish Vaswani, Noam Shazeer, Niki Parmar, Jakob Uszkoreit, Llion Jones, Aidan N. Gomez, Łukasz Kaiser, and Illia Polosukhin. Attention is all you need, 2017.

[45] Ting Chen, Simon Kornblith, Mohammad Norouzi, and Geoffrey Hinton. A simple framework for contrastive learning of visual representations, 2020.

[46] Jean-Bastien Grill, Florian Strub, Florent Altché, Corentin Tallec, Pierre H. Richemond, Elena Buchatskaya, Carl Doersch, Bernardo Avila Pires, Zhaohan Daniel Guo, Mohammad Gheshlaghi Azar, Bilal Piot, Koray Kavukcuoglu, Rémi Munos, and Michal Valko. Bootstrap your own latent: A new approach to self-supervised learning, 2020.

[47] Aaron van den Oord, Yazhe Li, and Oriol Vinyals. Representation learning with contrastive predictive coding, 2018.

[48] Jonathon Shlens. Notes on kullback-leibler divergence and likelihood, 2014.

[49] Joao Carreira and Andrew Zisserman. Quo vadis, action recognition? a new model and the kinetics dataset, 2018.

[50] OpenAI, Josh Achiam, Steven Adler, Sandhini Agarwal, Lama Ahmad, Ilge Akkaya, Florencia Leoni Aleman, Diogo Almeida, Janko Altenschmidt, Sam Altman, Shyamal Anadkat, Red Avila, Igor Babuschkin, Suchir Balaji, Valerie Balcom, Paul Baltescu, Haiming Bao, Mohammad Bavarian, Jeff Belgum, Irwan Bello, Jake Berdine, Gabriel Bernadett-Shapiro, Christopher Berner, Lenny Bogdonoff, Oleg Boiko, Madelaine Boyd, Anna-Luisa Brakman, Greg Brockman, Tim Brooks, Miles Brundage, Kevin Button, Trevor Cai, Rosie Campbell, Andrew Cann, Brittany Carey, Chelsea Carlson, Rory Carmichael, Brooke Chan, Che Chang, Fotis Chantzis, Derek Chen, Sully Chen, Ruby Chen, Jason Chen, Mark Chen, Ben Chess, Chester Cho, Casey Chu, Hyung Won Chung, Dave Cummings, Jeremiah Currier, Yunxing Dai, Cory Decareaux, Thomas Degry, Noah Deutscher, Damien Deville, Arka Dhar, David Dohan, Steve Dowling, Sheila Dunning, Adrien Ecoffet, Atty Eleti, Tyna Eloundou, David Farhi, Liam Fedus, Niko Felix, Simón Posada Fishman, Juston Forte, Isabella Fulford, Leo Gao, Elie Georges, Christian Gibson, Vik Goel, Tarun Gogineni, Gabriel Goh, Rapha Gontijo-Lopes, Jonathan Gordon, Morgan Grafstein, Scott Gray, Ryan Greene, Joshua Gross, Shixiang Shane Gu, Yufei Guo, Chris Hallacy, Jesse Han, Jeff Harris, Yuchen He, Mike Heaton, Johannes Heidecke, Chris Hesse, Alan Hickey, Wade Hickey, Peter Hoeschele, Brandon Houghton, Kenny Hsu, Shengli Hu, Xin Hu, Joost Huizinga, Shantanu Jain, Shawn Jain, Joanne Jang, Angela Jiang, Roger Jiang, Haozhun Jin, Denny Jin, Shino Jomoto, Billie Jonn, Heewoo Jun, Tomer Kaftan, Łukasz Kaiser, Ali Kamali, Ingmar Kanitscheider, Nitish Shirish Keskar, Tabarak Khan, Logan Kilpatrick, Jong Wook Kim, Christina Kim, Yongjik Kim, Jan Hendrik Kirchner, Jamie Kiros, Matt Knight, Daniel Kokotajlo, Łukasz Kondraciuk, Andrew Kondrich, Aris Konstantinidis, Kyle Kosic, Gretchen Krueger, Vishal Kuo, Michael Lampe, Ikai Lan, Teddy Lee, Jan Leike, Jade Leung, Daniel Levy, Chak Ming Li, Rachel Lim, Molly Lin, Stephanie Lin, Mateusz Litwin, Theresa Lopez, Ryan Lowe, Patricia Lue, Anna Makanju, Kim Malfacini, Sam Manning, Todor Markov, Yaniv Markovski, Bianca Martin, Katie Mayer, Andrew Mayne, Bob McGrew, Scott Mayer McKinney, Christine McLeavey, Paul McMillan, Jake McNeil, David Medina, Aalok Mehta, Jacob Menick, Luke Metz, Andrey Mishchenko, Pamela Mishkin, Vinnie Monaco, Evan Morikawa, Daniel Mossing, Tong Mu, Mira Murati, Oleg Murk, David Mély, Ashvin Nair, Reiichiro Nakano, Rajeev Nayak, Arvind Neelakantan, Richard Ngo, Hyeonwoo Noh, Long Ouyang, Cullen O’Keefe, Jakub Pachocki, Alex Paino, Joe Palermo, Ashley

Pantuliano, Giambattista Parascandolo, Joel Parish, Emy Parparita, Alex Passos, Mikhail Pavlov, Andrew Peng, Adam Perelman, Filipe de Avila Belbute Peres, Michael Petrov, Henrique Ponde de Oliveira Pinto, Michael, Pokorny, Michelle Pokrass, Vitchyr H. Pong, Tolly Powell, Alethea Power, Boris Power, Elizabeth Proehl, Raul Puri, Alec Radford, Jack Rae, Aditya Ramesh, Cameron Raymond, Francis Real, Kendra Rimbach, Carl Ross, Bob Rotsted, Henri Roussez, Nick Ryder, Mario Saltarelli, Ted Sanders, Shibani Santurkar, Girish Sastry, Heather Schmidt, David Schnurr, John Schulman, Daniel Selsam, Kyla Sheppard, Toki Sherbakov, Jessica Shieh, Sarah Shoker, Pranav Shyam, Szymon Sidor, Eric Sigler, Maddie Simens, Jordan Sitkin, Katarina Slama, Ian Sohl, Benjamin Sokolowsky, Yang Song, Natalie Staudacher, Felipe Petroski Such, Natalie Summers, Ilya Sutskever, Jie Tang, Nikolas Tezak, Madeleine B. Thompson, Phil Tillet, Amin Tootoonchian, Elizabeth Tseng, Preston Tuggle, Nick Turley, Jerry Tworek, Juan Felipe Cerón Uribe, Andrea Vallone, Arun Vijayvergiya, Chelsea Voss, Carroll Wainwright, Justin Jay Wang, Alvin Wang, Ben Wang, Jonathan Ward, Jason Wei, CJ Weinmann, Akila Welihinda, Peter Welinder, Jiayi Weng, Lilian Weng, Matt Wiethoff, Dave Willner, Clemens Winter, Samuel Wolrich, Hannah Wong, Lauren Workman, Sherwin Wu, Jeff Wu, Michael Wu, Kai Xiao, Tao Xu, Sarah Yoo, Kevin Yu, Qiming Yuan, Wojciech Zaremba, Rowan Zellers, Chong Zhang, Marvin Zhang, Shengjia Zhao, Tianhao Zheng, Juntang Zhuang, William Zhuk, and Barret Zoph. Gpt-4 technical report, 2024.

- [51] Adam Paszke, Sam Gross, Francisco Massa, Adam Lerer, James Bradbury, Gregory Chanan, Trevor Killeen, Zeming Lin, Natalia Gimelshein, Luca Antiga, Alban Desmaison, Andreas Köpf, Edward Yang, Zach DeVito, Martin Raison, Alykhan Tejani, Sasank Chilamkurthy, Benoit Steiner, Lu Fang, Junjie Bai, and Soumith Chintala. Pytorch: An imperative style, high-performance deep learning library, 2019.
- [52] Zoya Bylinskii, Tilke Judd, Aude Oliva, Antonio Torralba, and Frédo Durand. What do different evaluation metrics tell us about saliency models?, 2017.
- [53] Xinlei Chen, Hao Fang, Tsung-Yi Lin, Ramakrishna Vedantam, Saurabh Gupta, Piotr Dollar, and C. Lawrence Zitnick. Microsoft coco captions: Data collection and evaluation server, 2015.
- [54] Xuebin Qin, Zichen Zhang, Chenyang Huang, Masood Dehghan, Osmar Zaiane, and Martin Jagersand. U2-net: Going deeper with nested u-structure for salient object detection. volume 106, page 107404, 2020.
- [55] Youwei Pang, Xiaoqi Zhao, Lihe Zhang, and Huchuan Lu. Multi-scale interactive network for salient object detection, 2020.
- [56] Han Tian, Tao Deng, and Hongmei Yan. Driving as well as on a sunny day? predicting driver's fixation in rainy weather conditions via a dual-branch visual model. *IEEE/CAA Journal of Automatica Sinica*, 9(7):1335–1338, 2022.
- [57] Liang-Chieh Chen, George Papandreou, Florian Schroff, and Hartwig Adam. Rethinking atrous convolution for semantic image segmentation, 2017.
- [58] Shuai Bai, Keqin Chen, Xuejing Liu, Jialin Wang, Wenbin Ge, Sibo Song, Kai Dang, Peng Wang, Shijie Wang, Jun Tang, Humen Zhong, Yuanzhi Zhu, Mingkun Yang, Zhaohai Li, Jianqiang Wan, Pengfei Wang, Wei Ding, Zheren Fu, Yiheng Xu, Jiabo Ye, Xi Zhang, Tianbao Xie, Zesen Cheng, Hang Zhang, Zhibo Yang, Haiyang Xu, and Junyang Lin. Qwen2.5-v1 technical report, 2025.
- [59] Akis Linardos, Matthias Kümmeler, Ori Press, and Matthias Bethge. Deepgaze iie: Calibrated prediction in and out-of-domain for state-of-the-art saliency modeling, 2021.
- [60] Samuel F. Dodge and Lina J. Karam. Visual saliency prediction using a mixture of deep neural networks. *IEEE Transactions on Image Processing*, 27(8):4080–4090, 2018.
- [61] Matthias Kümmeler, Lucas Theis, and Matthias Bethge. Deep gaze i: Boosting saliency prediction with feature maps trained on imagenet, 2015.